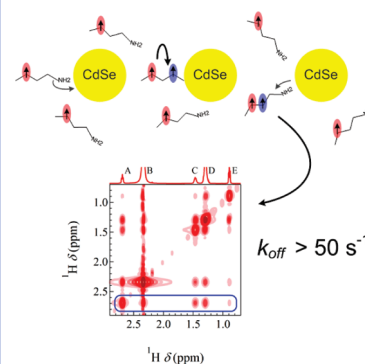


# Nuclear Magnetic Resonance Spectroscopy Demonstrating Dynamic Stabilization of CdSe Quantum Dots by Alkylamines

Antti Hassinen,<sup>†</sup> Iwan Moreels,<sup>†</sup> Celso de Mello Donegá,<sup>‡</sup> José C. Martins,<sup>§</sup> and Zeger Hens<sup>\*†</sup><sup>†</sup>Physics and Chemistry of Nanostructures, Ghent University, Belgium, <sup>‡</sup>Condensed Matter and Interfaces, Debye Institute, Utrecht University, The Netherlands, and <sup>§</sup>NMR and Structural Analysis Unit, Ghent University, Belgium

**ABSTRACT** The exchange kinetics of octylamine between a free state and a state bound to the surface of CdSe quantum dots is analyzed using nuclear magnetic resonance (NMR) spectroscopy in solution. On the basis of 1D <sup>1</sup>H and DOSY and NOESY spectroscopy, we find that all octylamine molecules present interact with the CdSe quantum dot surface, although the octylamine resonances and diffusion coefficient resemble those of free octylamine. This indicates that these NMR observables are a weighted average of a free and a bound state, implying that the overall octylamine exchange rate is fast as compared to the intrinsic NMR time scale. A lower limit on the first-order desorption rate constant of 50 s<sup>-1</sup> follows from DOSY measurements as a function of the diffusion delay. This result is compared with literature data based on the quenching of the CdSe photoluminescence upon alkylamine desorption.

**SECTION** Nanoparticles and Nanostructures



Ligands provide physicochemical functionality to colloidal nanoparticles (NPs). Used during synthesis to control nucleation and growth, they end up as a monolayer covering the NP surface and stabilizing the NP colloidal dispersion. After synthesis, they can be exchanged by others, and this has proven to be a powerful method to functionalize colloidal NPs, with the aim of, for example, raising their photoluminescence quantum yield,<sup>1</sup> rendering them biocompatible and bioselective<sup>2,3</sup> or enhancing their conductivity for applications in electronics<sup>4,5</sup> and photovoltaics.<sup>6</sup> In line with the increasing importance of NP ligands, a number of studies have addressed the interaction between ligands and NPs, and at the same time, a number of experimental techniques like nuclear magnetic resonance spectroscopy (NMR),<sup>7–10</sup> infrared spectroscopy,<sup>11</sup> or photoluminescence spectroscopy<sup>1,12–14</sup> were developed to investigate ligands bound to colloidal NPs.

An interesting model system in this respect is CdSe quantum dots (Q-CdSe) stabilized by alkylamines. It has been shown by a number of authors that alkylamines strongly enhance the Q-CdSe photoluminescence (PL).<sup>1,12,15</sup> On the basis of this, the increase or decrease of the Q-CdSe PL intensity has been interpreted in terms of an increased or reduced surface coverage by alkylamines, which means that the PL quantum yield is used as an indirect probe of the ligand surface coverage.<sup>12</sup> As a result, a number of adsorption isotherms and rate constants for desorption have been published. With desorption rates ranging from 0.01 to 1.5 × 10<sup>-4</sup> s<sup>-1</sup>,<sup>1,12</sup> all of these studies point toward a dynamic yet relatively strong binding of alkylamines to Q-CdSe. This contrasts with the fast exchange rates determined in a NMR spectroscopy

study on Q-CdTe stabilized by dodecylamine (DDA) and on Q-ZnO stabilized by octylamine (OctA).<sup>16</sup> In both cases, the QDs are observed to be dynamically stabilized by alkylamines, with an overall exchange rate exceeding 100 s<sup>-1</sup> for Q-CdTe. In contrast to PL spectroscopy, NMR can directly address the ligands. Apart from simply identifying and quantifying colloidal NP ligands, it also enables a direct assessment of their exchange behavior, which is classified as fast, intermediate, or slow relative to the relevant NMR time scale. Given the discrepancy in the exchange rates of alkylamines for Q-CdSe, based on PL,<sup>12</sup> and Q-CdTe, based on NMR,<sup>16</sup> we present in this Letter a NMR study of Q-CdSe stabilized by OctA that focuses on the ligand exchange regime.

CdSe QDs were synthesized in a mixture of hexadecylamine (HDA), trioctylphosphine (TOP), and trioctylphosphine oxide (TOPO), with dimethylcadmium and TOP-Se as the Cd and Se precursors, respectively.<sup>17</sup> Two samples were studied, with average QD diameters of 4.4 (sample A) and 3.9 nm (sample B). The <sup>1</sup>H NMR spectrum of the singly washed stock solution (see Experimental Section) shows mainly unbound TOPO (Figure 1). The presence of phosphorus-containing species is confirmed by a <sup>31</sup>P NMR spectrum, where we observe signals at 21.2 and 42.4 ppm, corresponding to TOP-Se<sup>18</sup> and TOPO,<sup>9</sup> respectively (see Supporting Information). The α-CH<sub>2</sub> protons of HDA, which are located at 2.5 ppm in a

Received Date: June 8, 2010

Accepted Date: August 10, 2010

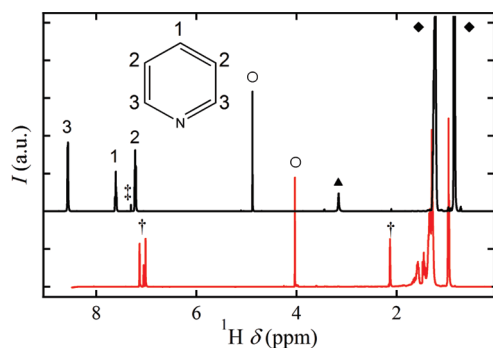


**Figure 1.**  $^1\text{H}$  NMR spectra of Q-CdSe capped with the original ligands in toluene- $d_8$  (bottom) and after pyridine ligand exchange in  $\text{CDCl}_3$  (top). Apart from the resonances of trioctylphosphine oxide (TOPO) between 1.0 and 1.6 ppm, the bottom spectrum shows resonances attributed to residual toluene- $d_8$  ( $\dagger$ ) and  $\text{CH}_2\text{Br}_2$  ( $\circ$ ), which was added as a concentration standard. The resonances in the top spectrum are attributed to residual  $\text{CDCl}_3$  ( $\ddagger$ ), hexane ( $\blacklozenge$ ), which results from the sample preparation, a pool of labile hydrogens ( $\blacktriangle$ ),  $\text{CH}_2\text{Br}_2$  ( $\circ$ ), which was added as a concentration standard, and finally pyridine. The pyridine resonances are numbered according to the inset. No trace of TOPO remains. From the figure, we conclude that the pyridine exchange completely removes the original ligands.

reference solution of HDA in tol- $d_8$ , are not observed in the CdSe QD sample. This indicates either the absence of HDA or the strong broadening of this resonance caused by the binding of HDA to the Q-CdSe surface.

To exchange these initial ligands for OctA, we follow Ji et al.<sup>12</sup> and use pyridine exchange as an intermediate step. Using deuterated chloroform ( $\text{CDCl}_3$ ) as a solvent, no resonances are observed in the aliphatic region (0.8–2.0 ppm) of the  $^1\text{H}$  NMR spectrum (Figure 1) after this exchange, except for those arising from hexane at 0.85 and 1.23 ppm, which is now used as a nonsolvent to precipitate the QDs. Instead, three somewhat broadened pyridine resonances appear in the spectral window from 7 to 9 ppm. A pool of labile hydrogens at 3.16 ppm is also present in the  $^1\text{H}$  NMR spectrum, possibly due to a minor contamination with water. Phosphorus-containing compounds were not observed in the  $^{31}\text{P}$  NMR, indicating the efficient removal of TOPO and TOP-Se, present in the original sample (see Supporting Information).

The broadening of the resonances already suggests that the pyridine is bound to the Q-CdSe. The interaction of pyridine with the colloidal NPs is confirmed by 2D nuclear Overhauser effect spectroscopy (NOESY). In NOESY, cross relaxation by dipolar coupling of neighboring protons leads to intense, negative cross peaks (NOEs) for large molecules, such as tightly bound ligands, while small molecules like free ligands only develop weak, positive NOEs. Importantly, ligands that only bind temporarily to the NP surface yield strong, negative NOE cross peaks similar to tightly bound ligands.<sup>16</sup> The 2D NOESY spectrum of pyridine-capped CdSe indeed shows these strong, negative NOE cross peaks for the pyridine resonances, which means that pyridine effectively acts as a ligand (see Supporting Information). However, diffusion-ordered spectroscopy (DOSY) on the pyridine-capped Q-CdSe yields a single diffusion coefficient of  $2.11 \times 10^{-9} \text{ m}^2/\text{s}$  for the pyridine resonances. For free

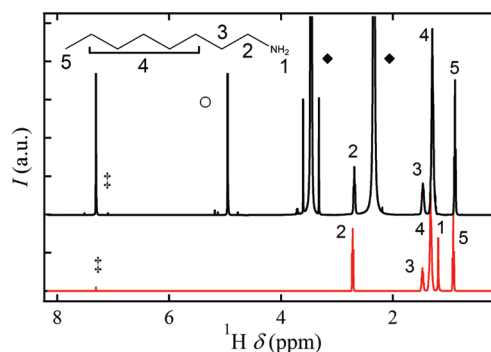


**Figure 2.**  $^1\text{H}$  NMR spectra of OctA (bottom) and Q-CdSe/OctA in  $\text{CDCl}_3$  (top). Resonances are attributed to residual  $\text{CDCl}_3$  ( $\ddagger$ ), methanol ( $\blacklozenge$ ), which was used during the ligand exchange,  $\text{CH}_2\text{Br}_2$  ( $\circ$ ), added as a concentration standard, and OctA (numbered according to the inset). For the peak assignment, see the Supporting Information. A comparison of both spectra shows that the OctA resonances in the Q-CdSe/OctA dispersion are only slightly broadened and shifted with respect to free OctA resonances.

pyridine, we found a diffusion coefficient of  $2.20 \times 10^{-9} \text{ m}^2/\text{s}$  in  $\text{CDCl}_3$  (see Supporting Information). This decrease by a mere 4% in the presence of the QDs and the absence of a slow diffusion component (on the order of  $10^{-10} \text{ m}^2/\text{s}$ ) suggest a dynamic adsorption/desorption equilibrium, where the bound pyridine is in fast exchange with a large excess of unbound pyridine present in the sample. The excess of free ligand is of course not unexpected as we have added 40–60  $\mu\text{L}$  of pyr- $d_5$  to prepare a stable suspension of Q-CdSe for the NMR measurements. This implies that on average,  $2.2 \times 10^5$  ligands are present for each QD. Assuming a typical ligand density of  $4 \text{ nm}^{-2}$ ,<sup>18</sup> this yields an estimated free/bound ligand ratio of 900:1.

Despite the large excess of pyridine, the  $^1\text{H}$  NMR spectrum of sample A in  $\text{CDCl}_3$  after the OctA ligand exchange demonstrates that the pyridine ligands are efficiently removed (Figure 2). Note that, in the preparation of the samples, it was crucial to prevent the precipitate from drying out completely. Consequently, methanol, which was used as a nonsolvent, is observed at 3.47 ( $\text{CH}_3$ ) and 2.34 ppm (OH). The OctA resonances appear at 2.69, 1.47, 1.30, and 0.89 ppm, and they are slightly broadened as compared to free OctA. The amine protons of the OctA most probably contribute to the pool of labile hydrogens at 2.34 ppm. In the 2D NOESY spectrum (Figure 3a), strong, negative NOE cross peaks are observed between the different OctA resonances. As in the case of the Q-CdSe–pyridine system, these negative cross peaks demonstrate that the OctA ligands spend time on the surface of the QDs. The labile hydrogens at 2.34 ppm also have negative NOE cross peaks with the OctA resonances, probably because the OH group of residual methanol and the  $\text{NH}_2$  group of OctA both contribute to this resonance. From DOSY, we obtain a single diffusion coefficient for all OctA resonances. It amounts to  $1.29 \times 10^{-9} \text{ m}^2/\text{s}$  for sample A and  $1.24 \times 10^{-9} \text{ m}^2/\text{s}$  for sample B. These values are merely 18 and 22% slower than the diffusion coefficient of free OctA in  $\text{CDCl}_3$  ( $1.59 \times 10^{-9} \text{ m}^2/\text{s}$ , Figure 3b), respectively, yet they considerably exceed the value expected for a particle with a hydrodynamic diameter of 4–5 nm. Similar to Q-CdTe/DDA,<sup>16</sup>

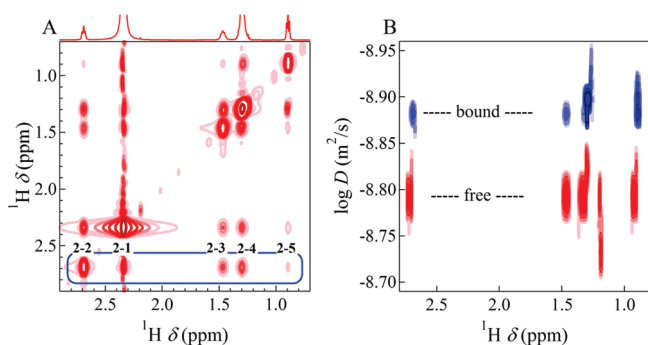


**Figure 3.** (a) Typical NOESY spectrum of Q-CdSe/OctA in  $\text{CDCl}_3$  using a 600 ms mixing time. Cross peaks (NOEs) starting from the diagonal  $\alpha\text{-CH}_2$  peak are indicated in the spectrum, where the numbers refer to the labeling introduced in Figure 2. The observation of strong negative NOEs demonstrates that OctA interacts with the Q-CdSe. (b) DOSY spectrum of free OctA (red) and Q-CdSe/OctA (blue) in  $\text{CDCl}_3$  using a diffusion delay of 50 ms. In the presence of Q-CdSe, OctA diffuses slower, yet the measured diffusion coefficient is larger than expected for tightly bound ligands. The combination of NOESY and DOSY points toward a fast adsorption/desorption equilibrium between free and bound OctA.

the 1D  $^1\text{H}$ , NOESY, and DOSY results all point toward a fast exchange of OctA between a free and a bound state, with an excess of free OctA. This excess of free OctA is confirmed by a quantitative  $^1\text{H}$  NMR spectrum. In the case of sample A, we calculate that on average 3000 ligands are present for each QD. Using again a ligand density of  $4\text{ nm}^{-2}$ ,<sup>18</sup> this corresponds to a free/bound ligand ratio of about 12:1. Importantly, due to the fast chemical exchange, the slightly broadened OctA  $^1\text{H}$  resonances represent exchange-averaged signals that are impossible to deconvolute to quantify the ratios of bound and free ligands.<sup>12</sup>

To demonstrate that every OctA ligand in the dispersion is involved in the exchange process, we analyzed the buildup of the NOE cross peak intensity as a function of the NOE mixing time. These buildup curves are described by

$$\frac{I_{AB}(t)}{I_{AA}(0)} = Ce^{-R_L t}(1 - e^{-R_C t}) \quad (1)$$

Here,  $I_{AB}(t)$  is the intensity of the NOE cross peak between resonance A and B at time  $t$ , and  $I_{AA}(0)$  is the initial intensity of the diagonal peak of resonance A, in this case associated with the  $\alpha\text{-CH}_2$  resonance.  $R_L$  is the overall  $T_1$  longitudinal relaxation rate describing the return to equilibrium, and  $R_C$  is the cross relaxation rate, giving rise to the NOE transfer. The prefactor  $C$  is the relative intensity that the NOE cross peak would attain if no longitudinal relaxation occurred. As such, it measures the fraction of the initial spin polarization of resonance A that is transferred to resonance B. By summing up this prefactor over all possible final resonances, we can estimate what fraction of the ligands is involved in the exchange process. Indeed, if no exchange takes place, the NOESY cross peak intensity will only be due to the fraction of bound ligands ( $f$ ). Starting then from the excitation of the  $\alpha\text{-CH}_2$ , the polarization from these 2  $\alpha\text{-CH}_2$  protons is transferred to all 17 other protons. Hence, a fraction  $17/19f$  of the initial spin polarization of the  $\alpha\text{-CH}_2$  will be transferred. Considering the 12:1 free/bound ligand ratio,

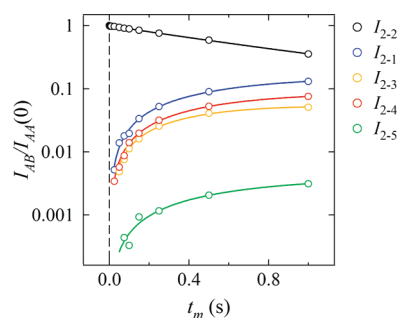


**Figure 4.** Open circles: buildup of the intensity of the NOE cross peaks as a function of the time span allowed for cross relaxation (mixing time  $t_m$ ). Full lines: best fits of the experimental data to eq 1, obtained using a fixed  $T_1$  relaxation time of 2.5 s. The subscripts denoting the respective peak intensities refer to the labels introduced in Figure 3a.

**Table 1.** Parameters Obtained from a Fit of the NOE Buildup Curves to Equation 1, Keeping the Transversal Relaxation Time ( $T_1$ ) Fixed at the Values Indicated<sup>a</sup>

	$T_1 = 2.5\text{ s}$		$T_1 = 3.0\text{ s}$	
	$C$	$1/R_C\text{ (s)}$	$C$	$1/R_C\text{ (s)}$
$I_{2-1}$	0.52(6)	2.2(3)	0.40(4)	1.6(2)
$I_{2-3}$	0.12(1)	0.91(8)	0.10(1)	0.78(7)
$I_{2-4}$	0.26(3)	1.8(2)	0.21(2)	1.4(2)
$I_{2-5}$	0.02(1)	3(1)	0.012(6)	2(1)

<sup>a</sup> Prefactor  $C$  gives the fraction of the initial spin polarization which is transferred from one resonance to other.  $R_C$  is the cross relaxation rate giving rise to the NOE transfer. As the sum of the prefactors is close to unity, we conclude that each OctA ligand in the Q-CdSe/OctA dispersion is involved in the rapid exchange process.

estimated from the quantitative NMR spectrum, we should observe a polarization transfer of 6.6% in this case. On the other hand, under conditions of fast exchange, all molecules spend time on the QD surface during the NOESY mixing time. Thus, all ligands contribute to the NOESY cross peaks, and a polarization transfer of 89% (i.e.,  $17/19$ ) may be expected.

The parameters resulting from a fit of the NOESY buildup curves to eq 1 depend on the actual value of the  $T_1$  relaxation time, which itself is hard to determine from the NOESY buildup. Therefore, we measured  $T_1$  independently for all OctA resonances (2.69, 1.47, 1.30, and 0.89 ppm), yielding values that varied between 2.5 and 3.1 s. As a result, we used fixed values of  $T_1$ , 2.5 and 3.0 s, to fit the NOE buildup curves (Figure 4). Apart from the transfer to the  $\text{CH}_3$  group ( $I_{2-5}$ ), this leads to well-defined fitting parameters (see Table 1), yielding an upper and a lower limit on the polarization transfer of about 90 and 70%, respectively. As outlined above, these high values confirm that essentially every OctA ligand in the Q-CdSe/OctA dispersion contributes to the negative NOE cross peak and thus spends time on the QD surface.

The disadvantage of a situation of rapid exchange in NMR is that it only yields a lower limit on the overall exchange rate  $k_{\text{on/off}}$ , which is defined for bimolecular exchange as<sup>16</sup>

$$k_{\text{on/off}} = k_{\text{off}} \left( 1 + \frac{x_{\text{bound}}}{x_{\text{free}}} \right) \quad (2)$$

**Table 2.** Diffusion Coefficients ( $D$ ) Obtained from the DOSY Measurements Using Different Diffusion Delays ( $\Delta$ )<sup>a</sup>

$\Delta$ (ms)	100	50	20
$D$ (m <sup>2</sup> /s)	$1.292 \pm 0.015 \times 10^{-9}$	$1.315 \pm 0.024 \times 10^{-9}$	$1.315 \pm 0.029 \times 10^{-9}$

<sup>a</sup> As a single, constant diffusion coefficient is obtained for delays down to 20 ms, we conclude that the exchange rate  $k_{\text{on/off}}$  strongly exceeds  $50 \text{ s}^{-1}$ .

Here,  $k_{\text{off}}$  is the first-order rate constant for desorption, while  $x_{\text{bound}}$  and  $x_{\text{free}}$  denote the molar fractions of bound and free ligands, respectively. Lower limits on  $k_{\text{on/off}}$  are most easily obtained from the DOSY spectra, where the transition between rapid and slow exchange — characterized by the appearance of two diffusion coefficients — occurs when the exchange rate is comparable to the inverse of the diffusion delay  $\Delta$ . We therefore performed DOSY measurements with a  $\Delta$  of 100, 50, and 20 ms. This always resulted in a single, constant diffusion coefficient, which demonstrates the occurrence of fast exchange in all cases (see Table 2). Given the excess of free ligands ( $x_{\text{free}}/x_{\text{bound}} \approx 0.08$ ), we conclude that the first-order rate constant  $k_{\text{off}}$  of OctA desorption strongly exceeds  $50 \text{ s}^{-1}$ . After reducing the temperature down to  $-40 \text{ }^\circ\text{C}$ , which is above the freezing point of  $\text{CDCl}_3$  ( $-64 \text{ }^\circ\text{C}$ ) but below the freezing point of neat OctA ( $-5 \text{ }^\circ\text{C}$ ), still no component with a small diffusion coefficient appeared in the DOSY spectrum ( $\Delta = 100 \text{ ms}$ ). Hence, even at these low temperatures, the fast dynamics persists, with a  $k_{\text{off}}$  exceeding  $10 \text{ s}^{-1}$ .

Summing up, the combination of 1D  $^1\text{H}$  spectroscopy, DOSY, and NOESY clearly shows that OctA molecules are dynamic ligands for Q-CdSe, exhibiting a rapid exchange between a bound and a free state with a desorption rate constant faster than  $50 \text{ s}^{-1}$ . This result is in line with previous work on the stabilization of Q-CdTe by DDA,<sup>16</sup> yet it is at odds with a number of literature studies on the thermodynamics and especially the kinetics of alkylamine exchange based on changes in PL quantum yield, which reported much slower ligand dynamics. Clearly, our results show that the relatively slow exchange rates deduced from studies of the PL intensity dynamics, with reported half-lives of 70 s up to 110 min,<sup>1,12</sup> cannot reflect the simple desorption of alkylamines. Indeed, an exchange rate of  $50 \text{ s}^{-1}$  or more implies that the entire ligand shell is refreshed at least 3500 times in a time span of 70 s. This indicates that the observed relationship between PL intensity and bound or free alkylamines is more complex than a mere proportionality between intensity and surface ligand coverage. The results reported here stress the importance of using direct analysis methods to address the interaction between ligands and colloidal NPs. In this respect, NMR spectroscopy has the advantage that it is an in situ technique that may give information on the kinetics and the thermodynamics of ligand exchange. If the exchange rate is faster than the inverse of the typical NMR time scales, it provides a lower limit on this exchange rate. However, as these conditions lead to averaged NMR observables, an accurate determination of the concentration of free and bound ligands is difficult, and thermodynamic information, such as adsorption isotherms and binding energies, is difficult to obtain. If the exchange rate is slow on the NMR time scales, bound and free

ligands can be observed separately. In the case of ligands forming a dative or dipolar bond, adsorption isotherms and binding energies can be determined under these conditions, as was shown for Q-InP/TOPO.<sup>19</sup>

## EXPERIMENTAL SECTION

Q-CdSe were prepared in a mixture of TOPO, TOP, and HDA. The synthesis is described in detail elsewhere.<sup>17</sup> The QD size is determined from the spectral position of the first absorption peak using the sizing curve of Jasieniak et al.<sup>20</sup> After synthesis, the QDs were washed once with methanol, dispersed in HDA, and kept under nitrogen. For the NMR experiments, the dispersions were purified by mixing them with toluene, precipitating with an excess of methanol, and redissolving the precipitate in toluene to produce a stock solution. For both samples, the particle concentration  $c_0$  was determined from the absorbance at 350 nm, using published values for the absorption coefficient.<sup>20</sup> Pyridine exchange was done following the procedure of Ji et al.<sup>12</sup> For NMR measurements, pyridine-capped particles were precipitated once more with an excess of hexane and dissolved in  $\text{CDCl}_3$ . In this last step, it was necessary to add a small amount of pyridine ( $40\text{--}60 \mu\text{L}$ ) to the sample and sonicate; otherwise, the precipitated QDs did not dissolve in  $\text{CDCl}_3$ . For the subsequent OctA exchange, the sample was precipitated, and the precipitate was dissolved in  $100 \mu\text{L}$  of OctA and  $350 \mu\text{L}$  of chloroform. The solution was sonicated for 10 min and precipitated by adding an excess of methanol. This OctA treatment was repeated once more. The final precipitate was dissolved in  $750 \mu\text{L}$  of  $\text{CDCl}_3$  to prepare a sample for NMR measurements. All  $^1\text{H}$  NMR spectra were collected using a Bruker Avance DRX 500 spectrometer ( $^1\text{H}$  and  $^{13}\text{C}$  frequencies of 500.13 and 125.76 MHz, respectively) equipped with a 5 mm TXI probe (maximum Z-gradient strength of  $0.535 \text{ T m}^{-1}$ ). The temperature was set to 298 K unless mentioned otherwise.

**SUPPORTING INFORMATION AVAILABLE** More detail on the experimental procedures and NMR spectroscopy ( $^1\text{H}$ , DOSY, NOESY, and  $^{31}\text{P}$ ). This material is available free of charge via the Internet at <http://pubs.acs.org>.

## AUTHOR INFORMATION

### Corresponding Author:

\*To whom correspondence should be addressed. Address: Physics and Chemistry of Nanostructures, Department of Inorganic and Physical Chemistry, Krijgslaan 281-S3, B-9000 Gent, Belgium. Tel: +32-9-2644863. Fax: +32-9-2644971. E-mail: Zeger.Hens@UGent.be.

**ACKNOWLEDGMENT** Z.H. thanks the Belgian Science Policy Office (IAP P6/10, photonics@be) and the European Community's Seventh Framework Program (EU-FP7 ITN Herodot under Grant Agreement No. 214954) for funding. The FWO Vlaanderen is thanked for funding to J.C.M. (G.0064.07 and G.0102.08) and to Z.H. and J.C.M. (G.0794.10). I.M. is a postdoctoral fellow of the FWO-Vlaanderen.

## REFERENCES

- (1) Bullen, C.; Mulvaney, P. The Effects of Chemisorption on the Luminescence of CdSe Quantum Dots. *Langmuir* **2006**, *22*, 3007–3013.

- (2) Medintz, I. L.; Uyeda, H. T.; Goldman, E. R.; Mattoussi, H. Quantum Dot Bioconjugates for Imaging, Labelling and Sensing. *Nat. Mater.* **2005**, *4*, 435–446.
- (3) Michalet, X.; Pinaud, F. F.; Bentolila, L. A.; Tsay, J. M.; Doose, S.; Li, J. J.; Sundaresan, G.; Wu, A. M.; Gambhir, S. S.; Weiss, S. Quantum Dots for Live Cells, In Vivo Imaging, and Diagnostics. *Science* **2005**, *307*, 538–544.
- (4) Talapin, D. V.; Murray, C. B. PbSe Nanocrystal Solids for n- and p-Channel Thin Film Field-Effect Transistors. *Science* **2005**, *310*, 86–89.
- (5) Kovalenko, M. V.; Scheele, M.; Talapin, D. V. Colloidal Nanocrystals with Molecular Metal Chalcogenide Surface Ligands. *Science* **2009**, *324*, 1417–1420.
- (6) Luther, J. M.; Law, M.; Beard, M. C.; Song, Q.; Reese, M. O.; Ellingson, R. J.; Nozik, A. J. Schottky Solar Cells Based on Colloidal Nanocrystal Films. *Nano Lett.* **2008**, *8*, 3488–3492.
- (7) Sachleben, J. R.; Colvin, V.; Emsley, L.; Wooten, E. W.; Alivisatos, A. P.; Solution-State, N. M. R. Studies of the Surface Structure and Dynamics of Semiconductor Nanocrystals. *J. Phys. Chem. B* **1998**, *102*, 10117–10128.
- (8) Kohlmann, O.; Steinmetz, W. E.; Mao, X. A.; Wuelfing, W. P.; Templeton, A. C.; Murray, R. W.; Johnson, C. S. NMR Diffusion, Relaxation, and Spectroscopic Studies of Water Soluble, Monolayer-Protected Gold Nanoclusters. *J. Phys. Chem. B* **2001**, *105*, 8801–8809.
- (9) Hens, Z.; Moreels, I.; Martins, J. C. In Situ <sup>1</sup>H NMR Study on the Trioctylphosphine Oxide Capping of Colloidal InP Nanocrystals. *ChemPhysChem* **2005**, *6*, 2578–2584.
- (10) Ribot, F.; Escax, V.; Roiland, C.; Sanchez, C.; Martins, J. C.; Biesemans, M.; Verbruggen, I.; Willem, R. In Situ Evaluation of Interfacial Affinity in CeO<sub>2</sub>-Based Hybrid Nanoparticles by Pulsed Field Gradient NMR. *Chem. Commun.* **2005**, 1019–1021.
- (11) von Holt, B.; Kudera, S.; Weiss, A.; Schrader, T. E.; Manna, L.; Parak, W. J.; Braun, M. Ligand Exchange of CdSe Nanocrystals Probed by Optical Spectroscopy in the Visible and Mid-IR. *J. Mater. Chem.* **2008**, *18*, 2728–2732.
- (12) Ji, X. H.; Copenhaver, D.; Sichmeller, C.; Peng, X. G. Ligand Bonding and Dynamics on Colloidal Nanocrystals at Room Temperature: The Case of Alkylamines on CdSe Nanocrystals. *J. Am. Chem. Soc.* **2008**, *130*, 5726–5735.
- (13) Koole, R.; Schapotschnikow, P.; Donega, C. D.; Vlugt, T. J. H.; Meijerink, A. Time-Dependent Photoluminescence Spectroscopy as a Tool to Measure the Ligand Exchange Kinetics on a Quantum Dot Surface. *ACS Nano* **2008**, *2*, 1703–1714.
- (14) Lorenz, J. K.; Ellis, A. B. Surfactant–Semiconductor Interfaces: Perturbation of the Photoluminescence of Bulk Cadmium Selenide by Adsorption of Tri-n-Octylphosphine Oxide as a Probe of Solution Aggregation with Relevance to Nanocrystal Stabilization. *J. Am. Chem. Soc.* **1998**, *120*, 10970–10975.
- (15) Munro, A. M.; Plante, I. J. L.; Ng, M. S.; Ginger, D. S. Quantitative Study of the Effects of Surface Ligand Concentration on CdSe Nanocrystal Photoluminescence. *J. Phys. Chem. C* **2007**, *111*, 6220–6227.
- (16) Fritzinger, B.; Moreels, I.; Lommens, P.; Koole, R.; Hens, Z.; Martins, J. C. In Situ Observation of Rapid Ligand Exchange in Colloidal Nanocrystal Suspensions Using Transfer NOE Nuclear Magnetic Resonance Spectroscopy. *J. Am. Chem. Soc.* **2009**, *131*, 3024–3032.
- (17) Donega, C. D.; Hickey, S. G.; Wuister, S. F.; Vanmaekelbergh, D.; Meijerink, A. Single-Step Synthesis to Control the Photoluminescence Quantum Yield and Size Dispersion of CdSe Nanocrystals. *J. Phys. Chem. B* **2003**, *107*, 489–496.
- (18) Moreels, I.; Fritzinger, B.; Martins, J. C.; Hens, Z. Surface Chemistry of Colloidal PbSe Nanocrystals. *J. Am. Chem. Soc.* **2008**, *130*, 15081–15086.
- (19) Moreels, I.; Martins, J. C.; Hens, Z. Ligand Adsorption/Desorption at Sterically Stabilized InP Colloidal Nanocrystals: Observation and Thermodynamic Analysis. *ChemPhysChem* **2006**, *7*, 1028–1031.
- (20) Jasieniak, J.; Smith, L.; van Embden, J.; Mulvaney, P. Re-Examination of the Size-Dependent Absorption Properties of CdSe Quantum Dots. *J. Phys. Chem. C* **2009**, *113*, 19468–19474.